4542–4551 *Nucleic Acids Research, 2007, Vol. 35, No. 13* *Published online 22 June 2007*
doi:10.1093/nar/gkm461

The abundance of RNPS1, a protein component of the exon junction complex, can determine the variability in efficiency of the Nonsense Mediated Decay pathway

Marcelo H. Viegas[1,2], Niels H. Gehring[1,2], Stephen Breit[1], Matthias W. Hentze[2,3] and Andreas E. Kulozik[1,2,*]

[1]Department of Pediatric Oncology, Hematology and Immunology, Children's Hospital, University of Heidelberg, Im Neuenheimer Feld 150, 69120 Heidelberg, Germany, [2]Molecular Medicine Partnership Unit (University of Heidelberg and European Molecular Biology Laboratory) and [3]European Molecular Biology Laboratory, Gene Expression Unit, Meyerhofstr 1, 69117 Heidelberg, Germany

Received February 13, 2007; Revised May 9, 2007; Accepted May 27, 2007

ABSTRACT

Nonsense-mediated mRNA decay (NMD) is a molecular pathway of mRNA surveillance that ensures rapid degradation of mRNAs containing premature translation termination codons (PTCs) in eukaryotes. NMD has been shown to also regulate normal gene expression and thus emerged as one of the key post-transcriptional mechanisms of gene regulation. Recently, NMD efficiency has been shown to vary between cell types and individuals thus implicating NMD as a modulator of genetic disease severity. We have now specifically analysed the molecular mechanism of variable NMD efficiency and first established an assay system for the quantification of NMD efficiency, which is based on carefully validated cellular NMD target transcripts. In a HeLa cell model system, NMD efficiency is shown to be remarkably variable and to represent a stable characteristic of different strains. In one of these strains, low NMD efficiency is shown to be functionally related to the reduced abundance of the exon junction component RNPS1. Furthermore, restoration of functional RNPS1 expression, but not of NMD-inactive mutant proteins, also restores efficient NMD in this model. We conclude that cellular concentrations of RNPS1 can modify NMD efficiency and propose that cell type specific co-factor availability represents a novel principle that controls NMD.

INTRODUCTION

Nonsense mediated decay (NMD) is a surveillance pathway by which cells recognize and limit the expression of mRNAs containing premature stop codons (PTCs) and thus reduce the expression of potentially harmful truncated proteins (1–4). Originally, NMD was thought to represent a control mechanism to limit the expression of faulty transcripts with frameshift or nonsense mutations, which originate from point mutations or from aberrant splicing. The finding of NMD being involved in negative feedback loops regulating normal gene expression foreshadowed a wider role of NMD as a basic post-transcriptional cellular process (5–7). More recently, microarray analyses of yeast (8,9), *Drosophila* (10) and human cells (11–13) have revealed that NMD modulates the levels of a large number of normal transcripts.

Furthermore, NMD has been suggested to vary in its efficiency. In *Saccharomyces cerevisiae*, the degradation of the pre-mRNA of CYH2 (an endogenous NMD target) has been reported to vary in different strains (14). In humans, the expression of dystrophin and *JARID1C* genes carrying identical nonsense mutations has been reported to differ and to modulate disease severity (15,16). Moreover, tissue-specific differences of NMD efficiency for nonsense-mutated collagen X have been suggested in a patient with Schmid metaphyseal chondrodysplasia (17). More recently, intertissue and interindividual variations in NMD efficiency have been proposed in the study of two fetuses diagnosed with Roberts syndrome and carrying a homozygous frameshift mutation in the *ESCO2* gene (18). These observations led to the hypothesis that variations of

*To whom correspondence should be addressed. Tel: +49 6221 56 2303; Fax: +49 6221 56 4559; Email: andreas.kulozik@med.uni-heidelberg.de
Correspondence may also be addressed to Matthias W. Hentze. Tel: +49 6221 387 501; Fax: +49 6221 387 518; Email: hentze@embl.de

NMD efficiency may contribute to the phenotypic variability of hereditary disorders (19,20). However, it has so far been difficult to quantify NMD efficiency.

Here, we have developed an assay system that estimates differences of NMD efficiency based on an internally controlled measurement of the expression of cellular NMD targets. Applying this assay in a HeLa cell model system we demonstrate variable NMD efficiency between strains. Functionally, these differences are shown to be caused by a deficiency of RNPS1, a key protein in at least one of the known NMD pathways (12). We thus propose that cell type specific co-factor availability represents a novel principle that controls NMD.

MATERIALS AND METHODS

Cell culture, transfections, RNA isolation and analysis

HeLa cells were grown in DMEM supplemented with 10% fetal calf serum (FCS) and 1% penicillin/streptomycin at 37°C and 5% CO_2. HeLa strain A has been used by our laboratory for many years (21,22). Strain B (ACC 57) was purchased at the German Repository of Cell lines (DSMZ). Strain C was kindly provided by Dr Elisa Izaurralde (EMBL, Heidelberg).

For plasmid and siRNA transfections, we used previously described methods (23). We isolated RNA according to standard protocols with TRIzol reagent (Invitrogen, CA, USA) and performed northern blot analysis as described previously (23) using 2–3 μg RNA per lane. Target sequences of siRNAs for luciferase, *UPF1* and *UPF2* were described previously (23). For estimations of mRNA half-life, actinomycinD (5 μg/ml) was added to the growth medium 48 h after siRNA treatment and RNA was collected every hour. Transcript abundance was quantified by quantitative RT-PCR as in the other cases. The half-life of the *FOS* transcript was used to monitor efficient inhibition of transcription.

Complementary RNA preparation and Microarray hybridization and analysis

We assessed the integrity of total cytoplasmic RNA from the cultured cells using a Agilent 2100 Bioanalyzer (Agilent, Palo Alto, CA, USA). We performed preparation, processing and hybridization of labelled and fragmented cRNA targets to Affymetrix HG_U133A GeneChips™ according to the manufacturer's protocols (Affymetrix Inc., Santa Clara, CA, USA). Oligonucleotide arrays were scanned using a confocal laser scanner (GeneArray™, Hewlett Packard, Palo Alto, CA, USA).

Statistical analysis of microarray data

Three independent experiments with *UPF1* siRNA or Luciferase siRNA as a negative control were analysed. We used the Affymetrix GeneChip Suite 5.0 software (MAS 5.0) to calculate raw expression values for each of the 22 283 probe sets on the U133A oligonucleotide array. Signal intensities were calculated as average intensity difference (AID) between perfect and mismatch probes. Approximately 8800 probe sets continuously resulting in absent calls were excluded from the analyses. Next, we used GeneSpring 4.2.1 (Silicon Genetics, Redwood City, CA, USA) for scaling, normalization and background correction of all genes and arrays. We performed Student's *t*-test on normalized relative expression ratios to identify significant differentially expressed genes with a minimum factor of difference of >2-fold, within the 95% confidence interval ($P < 0.05$). Full data sets are available in the Supplementary Data and on the Gene Expression Omnibus (GEO) repository (GSE7009).

Quantitative Real-Time PCR (LightCycler)

We synthesized first strand cDNA using MuMLV RNaseH- Reverse Transcriptase (MBI Fermentas) according to the manufacturer's protocol using 4 μg of RNA. We carried out real-time PCR, using the LightCycler system (Roche Diagnostics, Mannheim, Germany), as an independent method to assess differences of gene expression and to validate the microarray expression data. We performed expression analyses of selected genes with single-stranded cDNA and gene-specific primers (primer sequences are available on request). We used the FastStart DNA Master SYBR Green kit (Roche Diagnostics) to quantify the mRNA levels by measuring real-time fluorimetric intensity of SYBR green I incorporation. The working concentrations of gene-specific primer, $MgCl_2$, enzyme and SYBR green as well as cycling parameters were optimized according to the LightCycler protocol (LightCycler Operator's Manual, Version 3.5). For the experiments done in exclusively in strain A cells, we used the concentration of *glyceraldehyde-3-phosphate dehydrogenase* (*GAPDH*) to normalize all other genes tested from identical cDNA samples. For the other experiments also the *ribosomal protein L32* (*RPL32*), *hypoxanthine phosphoribosyltransferase 1* (*HPRT1*) and *core-binding factor-beta subunit* (*CBFB*) were included as standard controls. The ratio of each analysed cDNA was determined as the mean of 4 or 5 experiments. Melting curves of the PCR products were performed for quality control. The primer sequences of SC35 and GAPDH were described previously (12). For *TBL2*: gcagtcatttaccacatgc/tattgtttctgc ttcttggat, for *GADD45B*: gagtgagactgactgcaagc/tcttatta attcgcaaactgg, for *NAT9*: attgtgctggatgccgaga/acctagcgtg gtcactccgta, for *RPL32*: ttgacaacagggttcgtag/ttcttggaggaa acattgtg, for *HPRT1*: gaccagtcaacaggggacat/aacacttcgtgg ggtccttttc and for *CBFB*: gcccatctttacatacaca/acttcaaattat tactggctac.

Protein isolation and immunoblot analysis

We prepared protein lysates with an isotonic lysis buffer as described previously (23). For total extracts, the buffer composition was 50 mM Tris-HCl, pH 7.5, 150 mM NaCl,1 mM EDTA,1% Triton X-100, 0.5% Deoxycholate, 0.1% SDS,1× Complete protease inhibitor (Roche). For the cytoplasmic fraction, the buffer was 50 mM Tris-HCl, pH 7.2, 150 mM NaCl, 0.5% (v/v) NP-40, 0.1% Deoxycholate, 5 mM Vanadyl-Ribosyl-complex, 1 mM Dithiothreitol, 0.5 mM PMSF, 1× Complete protease inhibitor (Roche). We performed

immunoblot analysis of protein samples using 10–15 μg of total protein per lane as previously described (22).

Plasmid constructs

Plasmids for the expression of human β-globin WT and NS39 (22), Y14, RNPS1 and RNPS1Δ69-121 (12) and the loading control (23) were described previously.

RESULTS

Identification of *bona fide* cellular NMD targets

We aimed at developing an assay to estimate differences in NMD efficiency based on the expression levels of physiological NMD transcripts. To identify a panel of endogenous direct NMD targets in human cells, HeLa cells were treated with siRNA against the NMD-key factor *UPF1* (11,23,24) or Luciferase as a negative control. UPF1-specific immunoblotting showed that this protein was efficiently depleted to a level of <10% (Figure 1a). Functionally, the inhibition of NMD was assessed by monitoring the expression of (1) transfected nonsense mutated β-globin mRNA (NS39) (Figure 1b), and (2) of two known NMD-sensitive splice variants of *SC35* [*SFRS2*, referred to as SC35A and B (5)] (Figure 1c and d). In UPF1-depleted cells, both the β-globin NS39 reporter and the NMD sensitive *SC35* isoforms were up-modulated ~5- and 15-fold, respectively, demonstrating the effective inhibition of NMD. RNA isolated from these cells was analysed on Affymetrix HG_U133A GeneChips™. Of 22 283 probe sets, representing ~14 500 human genes, 9336 transcripts were expressed at a level of more than two SDs above background and were thus included in the analysis. A total of 265 probe sets (2.8%) representing 227 genes were up-modulated more than 2-fold, while 248 probe sets (2.6%) representing 202 genes were down-modulated more than 2-fold (Supplementary Data, Tables 1 and 2). These data indicate that a substantial number of genes are affected directly or indirectly by UPF1 activity.

In order to exclude transcripts that are affected by UPF1 depletion in an NMD-independent, non-post-transcriptional fashion, we analysed mRNA and pre-mRNA levels in a subset of 16 transcripts, chosen because of their strong differential expression in the microarray analyses. In several independent experiments performed on UPF1-depleted HeLa cells that showed efficiently inhibited NMD function (see Figure 1), pre-mRNA and mRNA levels for the selected 16 transcripts were quantified by RT-PCR (Figure 2). The microarray data showing up-regulated mRNA abundance in UPF1-depleted cells could be confirmed by RT-PCR for all 16 transcripts. However, only in the case of TBL2 the abundance of the pre-mRNA remained unchanged while the abundance of the mRNA was up-modulated ~8-fold. In the case of NAT9, these differences were marginal. In all other 14 RNAs, the abundance of the pre-mRNA and the mRNA did not differ significantly, although in two (*KCNJ12*, *SEPW1*) the pre-mRNA remained below the threshold of 2-fold up-regulation, whereas the mRNA was up-regulated to a level of >2-fold. These data suggest that

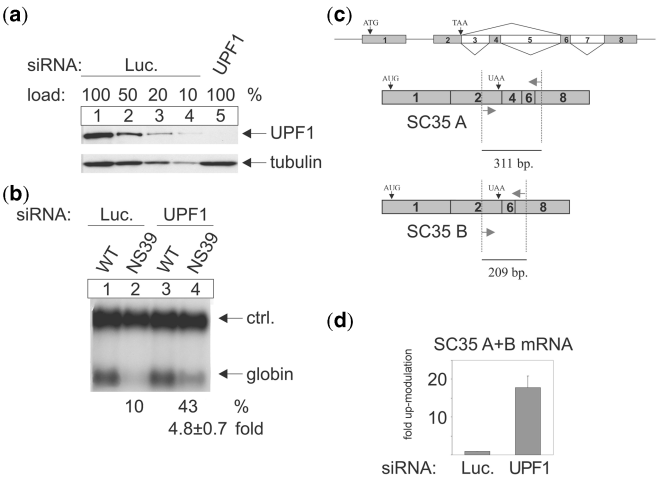

Figure 1. UPF1 depletion up-modulates the abundance of transfected and endogenous NMD reporters. (**a**) Immunoblot analysis of protein lysates from HeLa cells transfected with siRNAs against luciferase as a negative control or UPF1 using a UPF1-specific antibody. Serial dilutions corresponding to 100, 50, 20 or 10% (lanes 1–4) of the initial protein amount from luciferase-siRNA transfected cells were loaded to assess the efficiency of the UPF1 siRNA knock-down (lane 5). Reprobing with a tubulin-specific antibody was performed as a loading control. (**b**) HeLa cells were transfected with siRNAs against luciferase or UPF1. Thirty hours later, the cells were co-transfected with the β-globin WT or NS39 reporter constructs and the control plasmid. The indicated percentages correspond to the abundance levels of NS39 mRNAs compared to WT mRNAs after normalization for transfection efficiency (ctrl.). The fold up-regulation represents the ratio of NS39 expression levels between UPF1 and Luc siRNA transfected cells. Values and SEs were calculated from three independent experiments. (**c**) Gene structure of SC35 (SFRS2). Intron 1 is constitutively spliced, whereas exons 3 to 8 are subject to extensive alternative splicing. The position of the ATG and the stop codon are indicated. The exon composition of the two SC35 splice-variants, SC35 A and SC35 B that are subjected to NMD are shown below. The same pair of primers (arrows) was used to simultaneously amplify both species. (**d**) Quantitative RT-PCR analysis of the NMD-sensitive SC35 (SFRS2) variants in cells transfected with either UPF1 or luciferase siRNAs using the primers depicted in (c) and normalized against GAPDH expression. The mean and the SEs were calculated from five independent experiments.

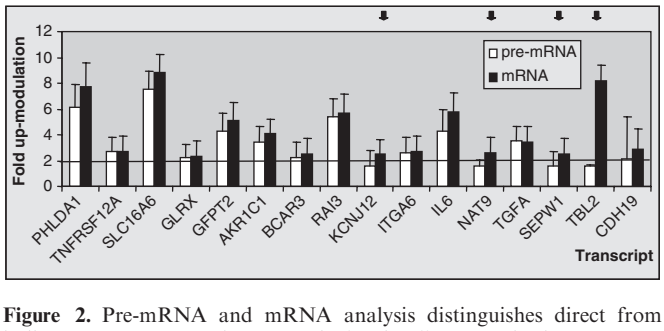

Figure 2. Pre-mRNA and mRNA analysis distinguishes direct from indirect NMD targets in UPF1-depleted cells. Quantitative RT-PCR (LightCycler) for 16 UPF1-sensitive transcripts from cells transfected with luciferase (negative control) or UPF1 siRNAs. The abundance of *glyceraldehyde-3-phosphate dehydrogenase* (*GAPDH*) was used for normalization. The fold up-modulation of pre-mRNAs and mRNAs by UPF1 depletion (mean ± SE) were calculated from 5–7 independent GAPDH normalized and LUC controlled experiments. Potential direct NMD targets (arrows) were defined as those mRNAs with a mean up-modulation >2-fold and with a mean pre-mRNA up-modulation <2-fold.

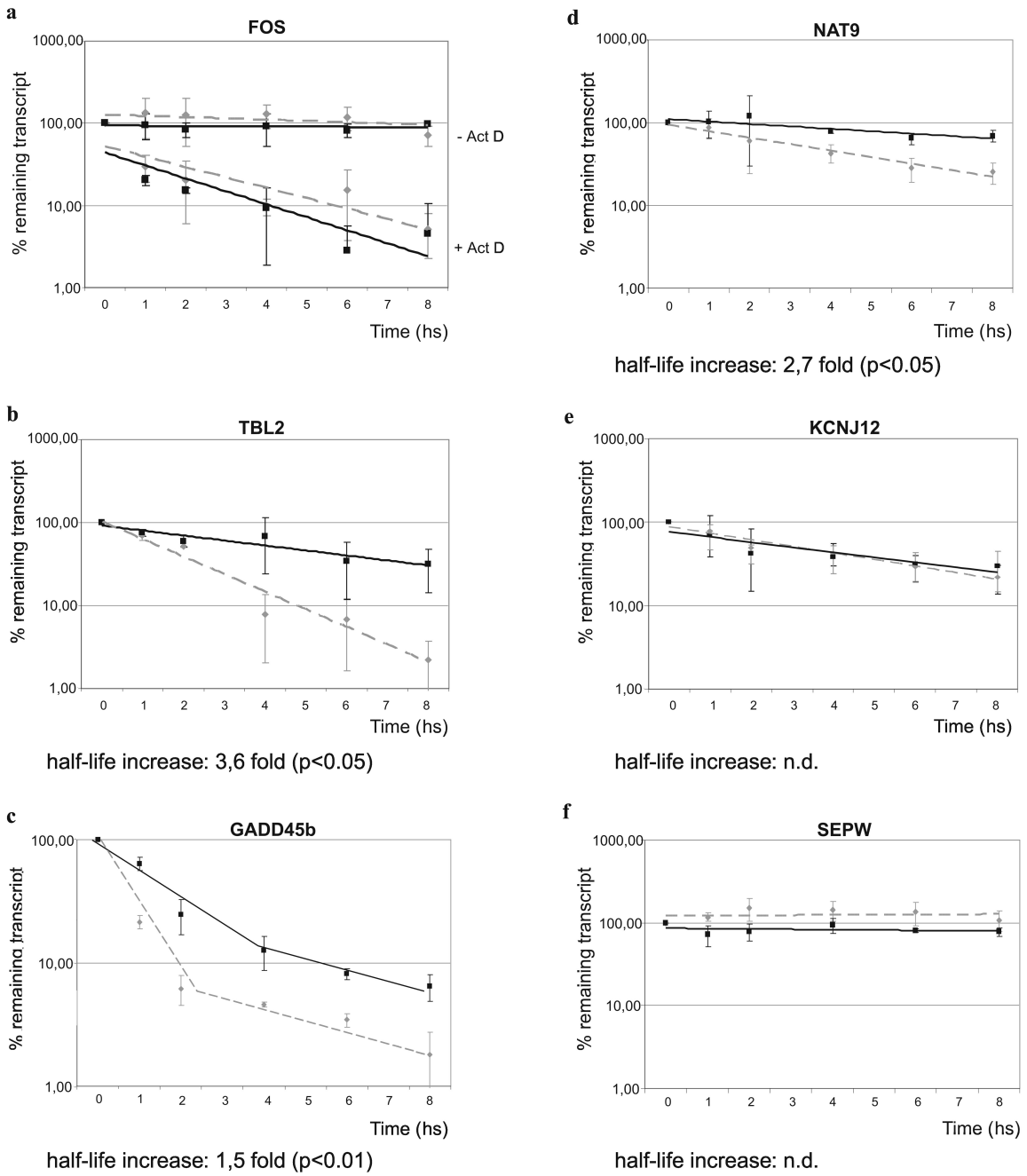

Figure 3. UPF1 depletion prolongs the half-lives of endogenous NMD targets. Decay rates of endogenous transcripts were measured in HeLa cells that were transfected with Upf1 siRNA (solid line) or Luciferase siRNA (dashed line) as control. 48 hours later, the cells were treated with actinomycin D (5μg/ml). Samples were taken every hour. mRNA levels were determined by RT-PCR quantification. The results represent the mean and standard deviation of three independent experiments. (**a**) The positive control FOS mRNA is stable in the absence of actinomycin D (−act.D) but it decays rapidly following a block of transcription (+act.D). (**b–f**) mRNA decay of the selected transcripts.

most of these mRNAs are likely up-modulated transcriptionally and do not represent *bona fide* NMD targets. By implication, these data also suggest that a substantial fraction, likely most of the almost 230 transcripts that are up-modulated by UPF1 depletion in our microarray data are indirect NMD targets.

Transcripts that are targeted by NMD are expected to be stabilized by an inhibition of this pathway. We thus analysed the decay rates of the *KCNJ12*, *NAT9*, *SEPW1* and *TBL2* mRNAs. We also included the *GADD45B* transcript, which has previously been suggested to represent an endogenous NMD target by *in silico* analysis (25) and is experimentally shown to be up-modulated by UPF1 depletion here (see below). Actinomycin D was added to cells pre-treated with siRNA against UPF1 or Luciferase. The short-lived *FOS* transcript was used as a positive control to assess the block of transcription (Figure 3a). Prolonged half-lives in UPF1-depleted cells

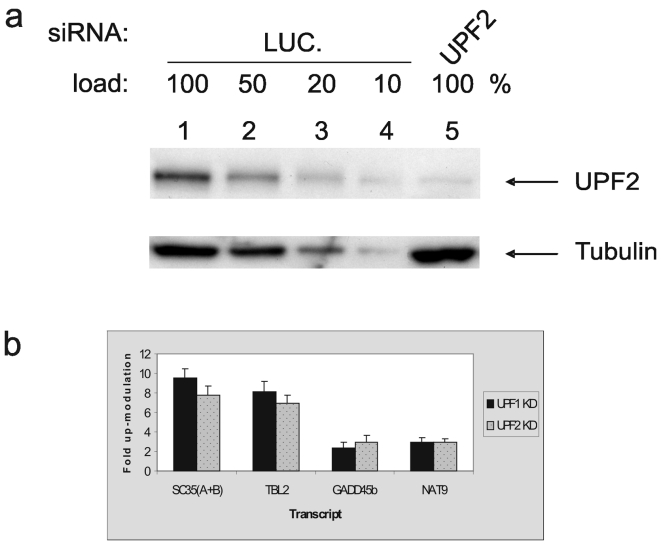

Figure 4. UPF1 and UPF2 depletion cause similar degrees of up-modulation of cellular NMD substrates. (**a**) Immunoblot analysis of protein lysates from HeLa cells transfected with siRNAs against luciferase as a negative control or UPF2 using a UPF2-specific antibody. Serial dilutions corresponding to 100, 50, 20 or 10% (lanes 1–4) of the initial protein amount from luciferase-siRNA transfected cells were loaded to assess the efficiency of the UPF2 siRNA depletion (lane 5). Reprobing with a tubulin-specific antibody was performed as a loading control. (**b**) Quantitative RT-PCR analysis of SC35 NMD-sensitive variants, TBL2, GADD45B and NAT9 in cells transfected with UPF1 or UPF2 siRNAs. The UPF1 and UPF2 siRNA treatments were controlled by luciferase siRNA and normalised against GAPDH. Mean and SEs were calculated from three independent experiments.

were detected for *GADD45B*, *TBL2* and *NAT9* confirming that UPF1 depletion increases the abundance of these transcripts by reducing degradation (Figure 3b–d). It is interesting to note that the degradation curve of the *GADD45B* transcript appears to be biphasic while those of the *TBL2* and *NAT9* transcripts appear to be monophasic. A biphasic decay curve for NMD substrates has been described previously (11,26,27) and can potentially be attributed to degradation of the nonsense-mutated mRNA during the first round of translation. Those mRNAs that escape degradation at that point are thought to be unaffected thereafter by NMD (28). The stability of *SEPW1* and *KCNJ12* did not show any effect on UPF1 depletion (Figure 3e–f). Because of this and because of the only marginal difference between pre-mRNA and mRNA levels (Figure 2), we excluded these transcripts from further analysis.

The role of NMD in directly modulating the abundance of the *TBL2*, *NAT9* and *GADD45B* transcripts was further analysed by depleting UPF2, which interacts with UPF1 in the NMD pathway (29,30). The efficient depletion of UPF2 to ~10% was confirmed by immunoblotting (Figure 4a) and, as a functional control, we assessed the abundance of *SC35*(A) and *SC35*(B) isoforms (referred to in the subsequent discussion as SC35). The degree of up-modulation in UPF1-depleted and UPF2-depleted cells was not significantly different for all four analysed transcripts (Figure 4b). Taken together, these results indicate that *SC35*, *TBL2*, *NAT9* and *GADD45B* are *bona fide* NMD targets that depend on both UPF1 and UPF2. Analysis of the structure of these transcripts using sequence databases show that SC35 (A and B), TBL2 and GADD45B possess a termination codon located more than 55 bases from the last exon–exon junction, while NAT9 contains an upstream open reading frame (uORF) (Supplementary Figure 1). These structural features are typical for cellular NMD targets (11,31), which may explain the sensitivity of these endogenous mRNAs to cellular NMD activity.

Different HeLa strains display remarkable variations in NMD efficiency

Unpublished observations in our laboratory have previously suggested that different strains of HeLa cells may differ in their NMD capacity. We have now used these HeLa strains as a model system to quantify subtle differences in NMD efficiency and to gain mechanistic insight into this variability.

The panel of five validated cellular NMD target transcripts (SC35 A + B, TBL2, NAT9 and GADD45B) was used to systematically analyse the NMD efficiency of three different HeLa cell strains (referred to as A, B and C). To avoid a potential bias of quantification against a single housekeeping gene, we selected four different transcripts (HPRT1, CBFB, GAPDH and RPL32) for normalisation purposes (32,33). This group of control transcripts was selected because (1) they showed <10% variability in all of our microarray experiments (data not shown); (2) they were expressed at different steady-state levels and (3) they belong to different metabolic pathways and are thus unlikely to be co-regulated. The comparison of the degree of up-modulation following UPF1 depletion showed similar results for all transcripts that were used for normalisation (Supplementary Figure 2), which indicated that all of these housekeeping genes can be used as standards.

Quantification of the five endogenous NMD targets (SC35 A + B combined, GADD45B, NAT9 and TBL2) against the four standards in these strains gave reproducible results in four independent experiments (Figure 5a). All the transcripts were ~2- to 3-fold significantly more abundant in strains B and C in comparison with strain A. Strain C showed a trend towards lower mean expression levels for the NMD targets than strain B, although these differences were not statistically significant. When the data from the individual NMD targets were combined, the same differences existed, which indicates the similar behaviour for all the tested mRNAs and suggests a stronger NMD capacity in cells of strain A (Figure 5b).

To validate our analysis, we estimated NMD efficiency by a direct comparison of the down-modulation of transfected, nonsense mutated β-globin (NS39) reporter in four independent experiments (Figure 5c and d). The down-modulation of the NS39 reporter differed reproducibly and significantly between strains. In strain A NMD efficiency was ~2.5-fold stronger than in the strains B and C, while strain C tended to be ~1.5-fold stronger than B. Thus, the quantification of NMD efficiency by

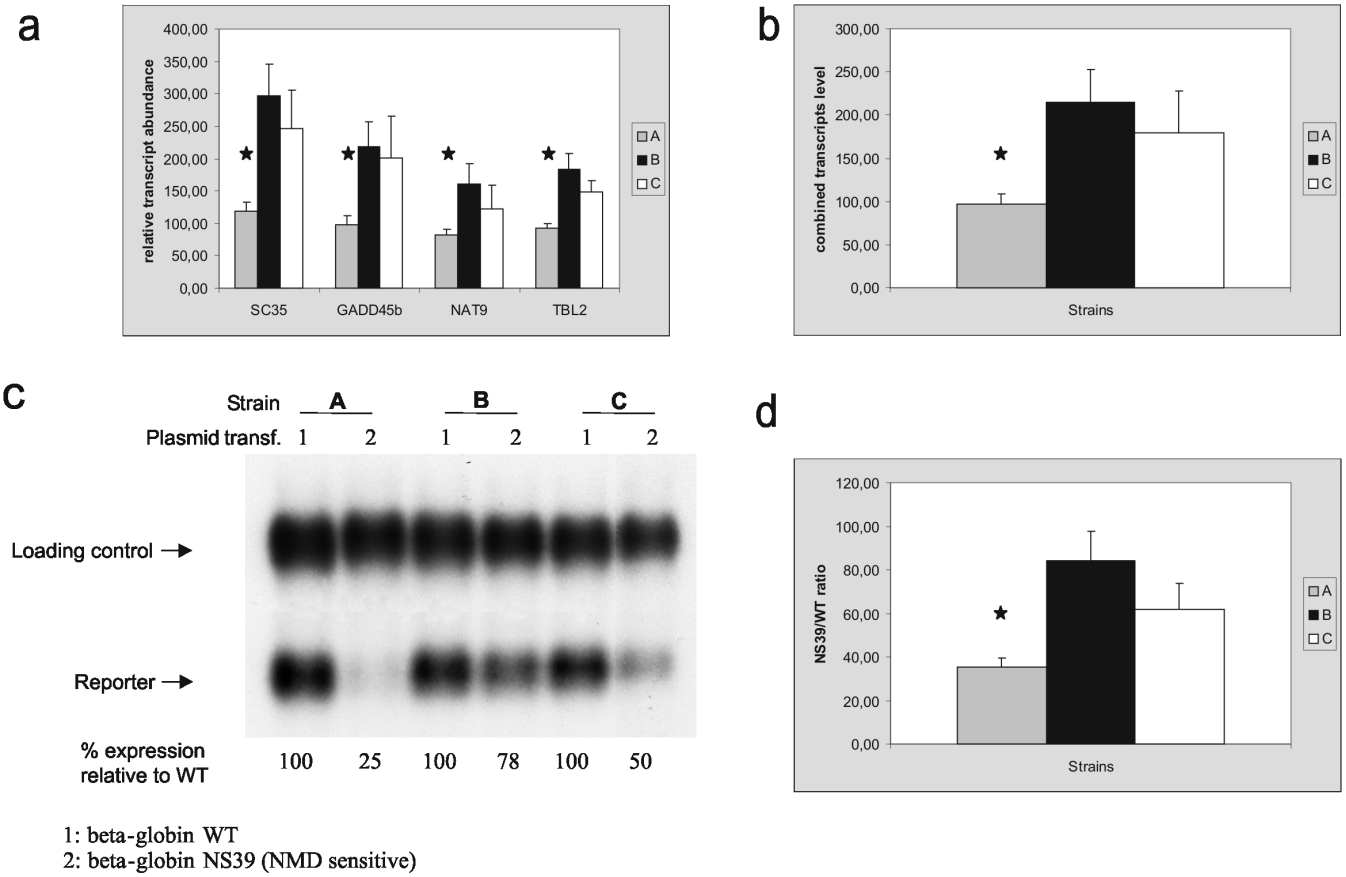

Figure 5. The abundance of cellular NMD targets reflects the variability of NMD efficiency in HeLa cell strains. (**a**) Quantification of five endogenous NMD transcripts (SC35 (A + B), GADD45B, NAT9 and TBL2) by real-time PCR in untransfected HeLa cells from three strains (A, B and C). The values plotted represent the mean plus SD of the quantification obtained using each of the four non-NMD targets for normalization in four independent experiments. For each NMD transcript, the expression levels are relative to the abundance of the transcript in strain A cells in one experiment arbitrarily set as 100. Significant differences ($P < 0.05$) are indicated with a star. (**b**) Means and SDs of the RNA abundance were pooled for the five NMD reporters (as shown in a). Significant differences ($P < 0.05$) are indicated with a star. (**c**) Representative northern blot of RNA from the three strains of HeLa cells that were transfected with β-globin WT or β-globin NS39. The quantification reflects the data from the individual experiment shown. (**d**) Quantification of the NS39/WT ratio for the northern blots analysis. The bar diagram expresses the mean and SD for three independent experiments.

analysis of cellular NMD target transcripts was confirmed by the independent analysis of the NS39 reporter.

These data demonstrate that differences of NMD efficiency between human cell lines can be estimated by measuring the abundance of transfected NMD-sensitive reporters and by analysing the abundance of a carefully validated panel of cellular NMD target transcripts.

RNPS1 abundance modulates NMD efficiency

Subsequently, we aimed at gaining insight into the mechanism of variable NMD efficiency in these HeLa strains. As a starting point, we analysed the abundance of the key NMD proteins UPF1, UPF2 and UPF3b and of the functionally critical exon junction complex components Y14, Magoh and RNPS1 by immunoblotting in both, total and cytoplasmic lysates (Figure 6a). The abundance of the UPF proteins, Y14 and Magoh did not differ between the three strains. In contrast, RNPS1 is shown to be less abundant in cells of strain B (Figure 6a). To estimate this difference semi-quantitatively, we compared the abundance of RNPS1 in lysates of cells of strain B relative to dilutions of similar lysates of cells of strain A and C. These results indicate that RNPS1 is ~50% less abundant in the cytoplasmic fraction in cells of strain B (Figure 6b, left panel). In total lysates, the abundance of RNPS1 in strain B is ~30% of that in strains A or C (Figure 6b, right panel).

We next functionally analysed if RNPS1 might be the limiting factor for NMD in these cells and over-expressed functional RNPS1 (12) in cells that were transfected with β-globin reporter genes. We confirmed that the transfection of pCI-NEO-Flag has no effect on the abundance of endogenous RNPS1 in any strain (Figure 7a, lower western blot) and that the pCI-NEO-RNPS1 is expressed at similar levels in the all three cell lines (Figure 7a, upper western blot). Increasing amounts of RNPS1 decreased the steady-state levels of the β-globin NS39 reporter up to 4-fold in cells of strain B but had no effect in cells of strains A and C (Figure 7a). This effect is specific for RNPS1, because over-expression of RNPS1Δ69-121

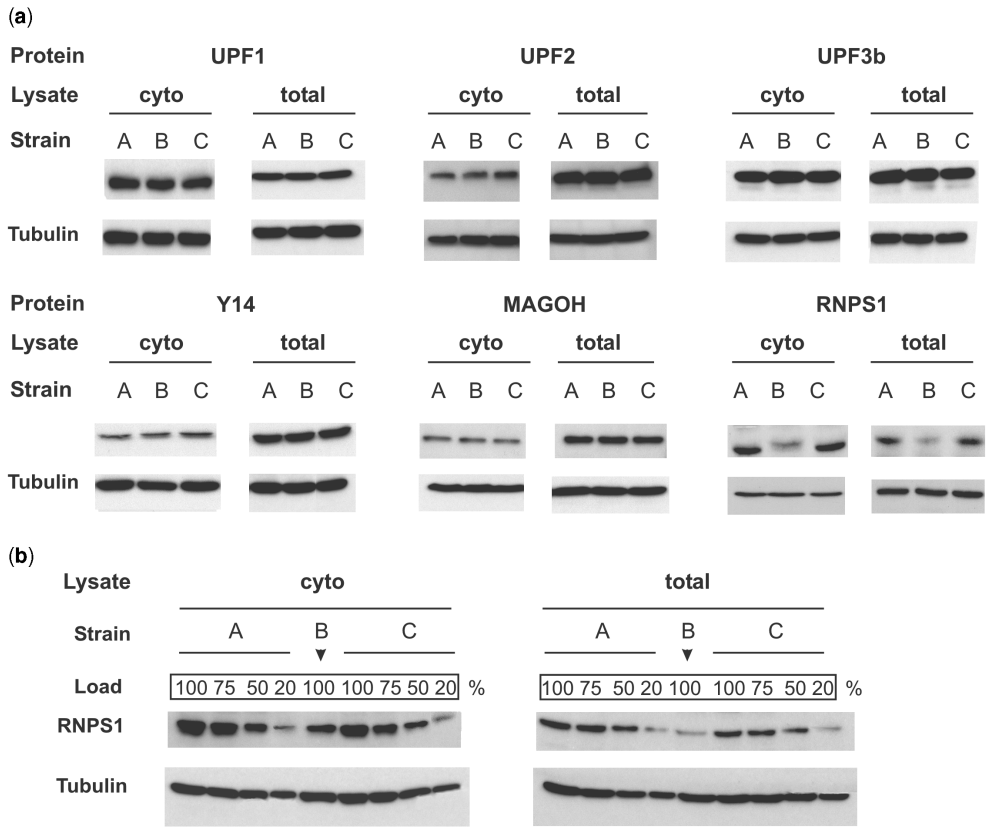

Figure 6. The low abundance of RNPS1 correlates with low NMD efficiency in one HeLa strain. (**a**) Representative western blots of cytoplasmic (cyto) and total lysates following staining with specific antibodies against UPF proteins, Y14, Magoh and RNPS1 in HeLa strains A,B and C. Reprobing with a tubulin-specific antibody was performed as a loading control. (**b**) Serial dilutions corresponding to 100, 75, 50 or 20% of the initial protein amount from cells of strain A and C were loaded to estimate the quantitative differences of RNPS1 abundance in cytoplasmic (cyto) or whole lysates of HeLa cells strain B.

(a truncated version of RNPS1 known to be non-functional in NMD (12)) does not affect the down-modulation of the NS39 reporter (Figure 7b). Furthermore, the over-expression of Y14—a critical EJC component for NMD function (23)—does not augment NMD efficiency in this strain of HeLa cells (Figure 7c). Based on the differences of RNPS1 abundance, the reconstitution of NMD efficiency by over-expression of a functional protein but not of a non-functional mutant and finally the lack of an effect of over-expressing another critical NMD protein, we conclude that the abundance of RNPS1 is limiting for NMD efficiency in HeLa strain B.

DISCUSSION

NMD has recently emerged as one of the critical post-transcriptional processes that regulate gene expression by targeting transcripts with truncated reading frames (9). While the phenomenon of variable NMD efficiency has been observed by many groups studying NMD (15–18,34), we document here that NMD efficiency can be systematically analysed by quantifying *bona fide* cellular NMD targets. Such cellular NMD targets have previously been thought to represent ~1–10% of the total transcriptome of human cells and yeast (9,11). However, our simultaneous analysis of pre-mRNA and mRNA abundance and of mRNA stability of selected transcripts (Figures 2 and 3) suggests that only a minority of UPF1-dependent transcripts are up-modulated directly by an inactivation of NMD. This apparently transcriptional effect of UPF1 depletion may be caused by influencing the expression of transcription factors either in an NMD-dependent fashion or in a fashion that is related to the non-NMD functions of UPF1 (35,36). This would indirectly affect the synthesis and the pre-mRNA abundance of target genes. Alternatively, the UPF1 depletion may stimulate the transcription of the up-modulated genes directly.

The five cellular NMD target mRNAs that were analysed (SC35A, SC35B and the identified TBL2, GADD45B and NAT9) here were also shown to be UPF2-sensitive (Figure 4) and to contain structural features (alternative splicing isoforms with premature stop codons and uORFs) (Supplementary Figure 1) that explain their NMD sensitivity. Interestingly, the quantification of this small set of carefully validated cellular NMD targets reflected subtle differences of NMD efficiency in different strains of the same cell line thus demonstrating that NMD efficiency can be measured semi-quantitatively. Such measurements may help to analyse NMD efficiency in more complex systems such as in tissues or even in entire organisms. However, the heterogeneity of the composition of such material will

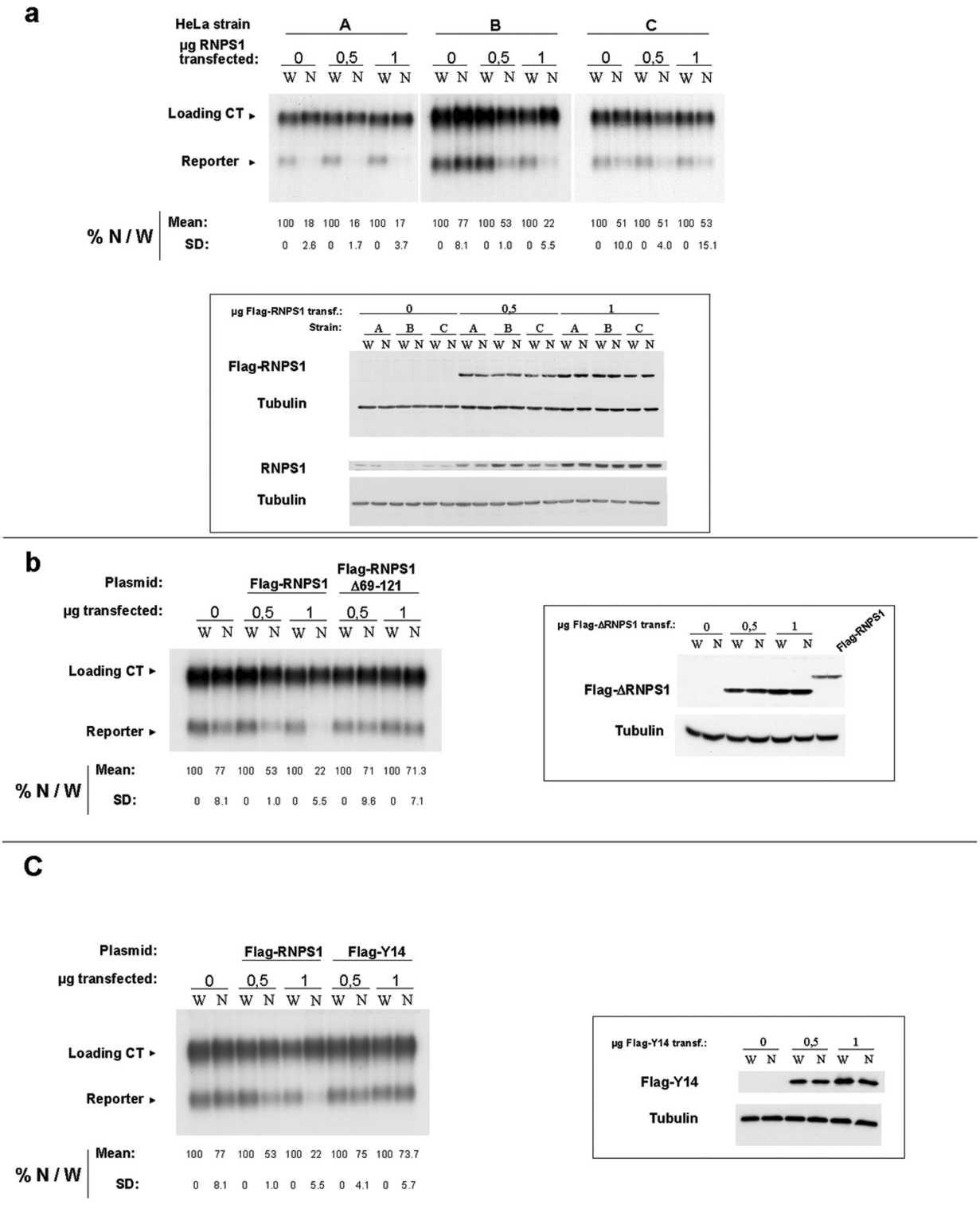

Figure 7. RNPS1 enhances NMD efficiency in one HeLa strain. (**a**) Upper panel: representative northern blot of RNA from the three strains of HeLa cells that were transfected with β-globin WT (W) or β-globin NS39 (N) and 0, 0.5 or 1 µg of pCI-NEO-FlagRNPS1. The quantification refers to mean values (Mean) and standard deviation (SD) of three independent experiments. Lower panel: western blots of lysates from transfected HeLa cells used in these experiments. The same extracts were run in two gels. After blotting, the upper membrane was probed using anti-flag antibody and the lower one was probed using anti-RNPS1 antibody. Both membranes were reprobed with anti-tubulin antibody to control the load. (**b**) Left: representative northern blot of RNA from strain B cells that were transfected with β-globin WT(W) or β-globin NS39 (N) and 0, 0.5 or 1 µg of pCI-NEO-FlagRNPS1 or pCI-NEO-FlagRNPS1Δ69-121 as a negative control. The quantification refers to mean values (Mean) and SD of three independent experiments. Right: western blot of transfected strain B HeLa cells. An anti-flag antibody was used to validate the expression of flag-RNPS1Δ69-121. As a further control, an extract of cells transfected with the full-length RNPS1 was also loaded. (**c**) Left: idem b) but transfecting pCI-NEO-FlagY14 as a negative control. Right: western blot for the transfected strain B HeLa cells. An anti-flag antibody was used to verify the expression of flag-Y14. The blot was reprobed with anti-tubulin to control the load.

have to be controlled as a likely confounding factor of such measurements.

NMD variability has previously been studied systematically only in yeast (14). The analysis of the yeast NMD substrate CYH2 pre-mRNA in strain crosses suggested that the variable efficiency of NMD is pleiotropic in this organism. Although we cannot discard a multi-gene effect to also be important in human cells, the findings reported here document that the abundance and functional availability of a single NMD co-factor can be limiting for NMD efficiency.

NMD is thought to require the interaction of the exon junction complex (EJC) with the SURF complex that is recruited to the ribosome at the site of translation termination (30). The EJC is recruited to the RNA by the spliceosome and is remodelled during nucleo-cytoplasmic export (37). Structural analyses have shown that the EJC is anchored to the RNA by a core that consists of the proteins eIF4AIII and MNL51 (BTZ) and the Y14/Magoh heterodimer (38,39). At the periphery of the complex, a number of other proteins are thought to establish the interaction of the EJC with other protein networks and different cellular functions (40,41). The protein RNPS1 is one of these peripheral EJC proteins that have previously been shown to activate the NMD pathway following tethering to a NMD competent position of the mRNA (23,42) and to be an important component of one of two pathways implicated in NMD (12). Interestingly, the data reported here now functionally link the reduced abundance of this protein in one of the cell lines to low NMD efficiency, thus for the first time implicating the natural abundance of an EJC protein to the efficiency of NMD.

SUPPLEMENTARY DATA

Supplementary Data are available at NAR Online.

ACKNOWLEDGEMENTS

We thank Dr. Elisa Izaurralde for providing HeLa cells (strain C). This work was funded by grants from the Fritz Thyssen Stiftung and the Deutsche Forschungsgemeinschaft (DFG).

Conflict of interest statement. None declared.

REFERENCES

1. Mango,S.E. (2001) Stop making nonSense: the *C. elegans* smg genes. *Trends Genet*., **17**, 646–53.
2. Gonzalez,C.I. *et al*. (2001) Nonsense-mediated mRNA decay in Saccharomyces cerevisiae. *Gene*, **274**, 15–25.
3. Gatfield,D. *et al*. (2003) Nonsense-mediated mRNA decay in Drosophila: at the intersection of the yeast and mammalian pathways. *EMBO J*., **22**, 3960–3970.
4. Maquat,L.E. (2004) Nonsense-mediated mRNA decay: splicing, translation and mRNP dynamics. *Nat. Rev. Mol. Cell Biol*., **5**, 89–99.
5. Sureau,A. *et al*. (2001) SC35 autoregulates its expression by promoting splicing events that destabilize its mRNAs. *EMBO J*., **20**, 1785–1796.
6. Wollerton,M.C. *et al*. (2004) Autoregulation of polypyrimidine tract binding protein by alternative splicing leading to nonsense-mediated decay. *Mol. Cell*, **13**, 91–100.
7. Mitrovich,Q.M. and Anderson,P. (2000) Unproductively spliced ribosomal protein mRNAs are natural targets of mRNA surveillance in *C. elegans*. *Genes Dev*., **14**, 2173–2184.
8. Lelivelt,M.J. and Culbertson,M.R. (1999a) Yeast upf proteins required for RNA surveillance affect global expression of the yeast transcriptome. *Mol. Cell. Biol*., **19**, 6710–6719.
9. He,F. *et al*. (2003) Genome-wide analysis of mRNAs regulated by the nonsense-mediated and 5′ to 3′ mRNA decay pathways in yeast. *Mol. Cell*, **12**, 1439–1452.
10. Rehwinkel,J. *et al*. (2005) Nonsense-mediated mRNA decay factors act in concert to regulate common mRNA targets. *RNA*, **11**, 1530–1544.
11. Mendell,J.T. *et al*. (2004) Nonsense surveillance regulates expression of diverse classes of mammalian transcripts and mutes genomic noise. *Nat. Genet*., **36**, 1073–1078.
12. Gehring,N.H. *et al*. (2005) Exon-junction complex components specify distinct routes of nonsense-mediated mRNA decay with differential cofactor requirements. *Mol. Cell*, **20**, 65–75.
13. Wittmann,J., Hol,E.M. and Jack,H.M. (2006) hUPF2 silencing identifies physiologic substrates of mammalian nonsense-mediated mRNA decay. *Mol. Cell Biol*., **26**, 1272–1287.
14. Kebaara,B. *et al*. (2003) Genetic background affects relative nonsense mRNA accumulation in wild-type and upf mutant yeast strains. *Curr. Genet*., **43**, 171–177.
15. Kerr,T.P. *et al*. (2001) Long mutant dystrophins and variable phenotypes: evasion of nonsense-mediated decay? *Hum. Genet*., **109**, 402–407.
16. Jensen,L.R. *et al*. (2005) Mutations in the JARID1C gene, which is involved in transcriptional regulation and chromatin remodeling, cause X-linked mental retardation. *Am. J. Hum. Genet*., **76**, 227–236.
17. Bateman,J.F. *et al*. (2003) Tissue-specific RNA surveillance? Nonsense-mediated mRNA decay causes collagen X haploinsufficiency in Schmid metaphyseal chondrodysplasia cartilage. *Hum. Mol. Genet*., **12**, 217–225.
18. Resta,N. *et al*. (2006) A homozygous frameshift mutation in the ESCO2 gene: evidence of intertissue and interindividual variation in Nmd efficiency. *J. Cell Physiol*., **209**, 67–73.
19. Frischmeyer,P.A. and Dietz,H.C. (1999) Nonsense-mediated mRNA decay in health and disease. *Hum. Mol. Genet*., **8**, 1893–1900.
20. Holbrook,J.A. *et al*. (2004) Nonsense-mediated decay approaches the clinic. *Nat. Genet*., **36**, 801–808.
21. Enssle,J. *et al*. (1993) Determination of mRNA fate by different RNA polymerase II promoters. *Proc. Natl Acad. Sci. USA*, **90**, 10091–10095.
22. Thermann,R. *et al*. (1998) Binary specification of nonsense codons by splicing and cytoplasmic translation. *EMBO J*., **17**, 3484–3494.
23. Gehring,N.H. *et al*. (2003) Y14 and hUpf3b form an NMD-activating complex. *Mol. Cell*, **11**, 939–949.
24. Mendell,J.T., ap Rhys,C.M. and Dietz,H.C. (2002) Separable roles for rent1/hUpf1 in altered splicing and decay of nonsense transcripts. *Science*, **298**, 419–422.
25. Hillman,R.T., Green,R.E. and Brenner,S.E. (2004) An unappreciated role for RNA surveillance. *Genome Biol*., **5**, R8.
26. Leeds,P. *et al*. (1992) Gene products that promote mRNA turnover in Saccharomyces cerevisiae. *Mol. Cell. Biol*., **12**, 2165–2177.
27. Guan,Q. *et al*. (2006) Impact of nonsense-mediated mRNA decay on the global expression profile of budding yeast. *PLoS Genet*., **2**, e203.
28. Ishigaki,Y. *et al*. (2001) Evidence for a pioneer round of mRNA translation: mRNAs subject to nonsense-mediated decay in mammalian cells are bound by CBP80 and CBP20. *Cell*, **106**, 607–617.
29. Singh,G. and Lykke-Andersen,J. (2003) New insights into the formation of active nonsense-mediated decay complexes. *Trends Biochem. Sci*., **28**, 464–466.
30. Kashima,I. *et al*. (2006) Binding of a novel SMG-1-Upf1-eRF1-eRF3 complex (SURF) to the exon junction complex triggers Upf1 phosphorylation and nonsense-mediated mRNA decay. *Genes Dev*., **20**, 355–367.

31. Nagy,E. and Maquat,L. (1998) A rule for termination-codon position within intron-containing genes: when nonsense affects RNA abundance. *Trends Biochem. Sci.*, **23**, 198–199.
32. Jin,P. *et al.* (2004) Selection and validation of endogenous reference genes using a high throughput approach. *BMC Genomics*, **5**, 55.
33. Zhang,X., Ding,L. and Sandford,A.J. (2005) Selection of reference genes for gene expression studies in human neutrophils by real-time PCR. *BMC Mol. Biol.*, **6**, 4.
34. Hutchinson,S. *et al.* (2003) Allelic variation in normal human FBN1 expression in a family with Marfan syndrome: a potential modifier of phenotype? *Hum. Mol. Genet.*, **12**, 2269–276. Epub 2003 Jul 22.
35. Kaygun,H. and Marzluff,W.F. (2005) Regulated degradation of replication-dependent histone mRNAs requires both ATR and Upf1. *Nat. Struct. Mol. Biol.*, **12**, 794–800.
36. Azzalin,C.M. and Lingner,J. (2006) The human RNA surveillance factor UPF1 is required for S phase progression and genome stability. *Curr. Biol.*, **16**, 433–439.
37. Ballut,L. *et al.* (2005) The exon junction core complex is locked onto RNA by inhibition of eIF4AIII ATPase activity. *Nat. Struct. Mol. Biol.*, **12**, 861–869. Epub 2005 Sep 18.
38. Bono,F. *et al.* (2006) The crystal structure of the exon junction complex reveals how it maintains a stable grip on mRNA. *Cell*, **126**, 713–725.
39. Andersen,C.B. *et al.* (2006) Structure of the exon junction core complex with a trapped DEAD-box ATPase bound to RNA. *Science*, **313**, 1968–1972.
40. Shibuya,T. *et al.* (2004) eIF4AIII binds spliced mRNA in the exon junction complex and is essential for nonsense-mediated decay. *Nat. Struct. Mol. Biol.*, **11**, 346–351. Epub 2004 Mar 21.
41. Tange,T.O. *et al.* (2005) Biochemical analysis of the EJC reveals two new factors and a stable tetrameric protein core. *RNA*, **11**, 1869–1883.
42. Lykke-Andersen,J., Shu,M.D. and Steitz,J.A. (2001) Communication of the position of exon-exon junctions to the mRNA surveillance machinery by the protein RNPS1. *Science*, **293**, 1836–1839.